

Superconducting phase diagram of the filled skutterudite PrOs₄Sb₁₂M.-A. Measson,¹ D. Braithwaite,¹ J. Flouquet,¹ G. Seyfarth,² J. P. Brison,² E. Lhotel,²
C. Paulsen,² H. Sugawara,³ and H. Sato³¹*Département de Recherche Fondamentale sur la Matière Condensée, SPSMS, CEA Grenoble, 38054 Grenoble, France*²*Centre de Recherches sur les Très basses températures, CNRS, 25 avenue des Martyrs, BP166, 38042 Grenoble CEDEX 9, France*³*Department of Physics, Tokyo Metropolitan University, Minami-Ohsawa 1-1, Hashioji, Tokyo 192-0397, Japan*

(Received 16 March 2004; published 27 August 2004)

We present new measurements of the specific heat of the heavy fermion superconductor PrOs₄Sb₁₂, on a sample which exhibits two sharp distinct anomalies at $T_{c1}=1.89$ K and $T_{c2}=1.72$ K. They are used to draw a precise magnetic field-temperature superconducting phase diagram of PrOs₄Sb₁₂ down to 350 mK. We discuss the superconducting phase diagram of PrOs₄Sb₁₂ and its possible relation with an unconventional superconducting order parameter. We give a detailed analysis of $H_{c2}(T)$, which shows the paramagnetic limitation (a support for even parity pairing) and multiband effects.

DOI: 10.1103/PhysRevB.70.064516

PACS number(s): 74.25.Dw, 65.40.Ba, 71.27.+a, 74.25.Op

I. INTRODUCTION

The first Pr-based heavy fermion (HF) superconductor PrOs₄Sb₁₂ ($T_c \sim 1.85$ K) has been recently discovered.¹ Evidence for its heavy fermion behavior is provided mainly by its superconducting properties, like the height of the specific heat jump at the superconducting transition or the high value of $H_{c2}(T)$ relative to T_c .¹ PrOs₄Sb₁₂ is cubic with T_h point group symmetry,² and has a nonmagnetic ground state, which in a single ion scheme can be either a Γ_{23} doublet or a Γ_1 singlet, a question which remains a matter of controversy. Presently, most measurements in high field seem to favor a singlet ground state.³⁻⁶ In any case, whatever the degeneracy of this ground state, the first excited state (at around 6 K) is low enough to allow for an induced electric quadrupolar moment on the Pr³⁺ ions,^{7,8} that could explain the heavy fermion properties of this system by a quadrupolar Kondo effect.¹ Thus, while the pairing mechanism of usual HF superconducting compounds (U or Ce-based) could come from magnetic fluctuations, the superconducting state of PrOs₄Sb₁₂ could be due to quadrupolar fluctuations. Yet at present, this attractive hypothesis is backed by very few experimental facts, both as regards the evidence of a quadrupolar Kondo effect in the normal phase and as regards the pairing mechanism in the superconducting state. Even the question of the unconventional nature of its superconductivity is still open. Indeed, several types of experiments have already probed the nature of this superconducting state, but with apparently contradictory results. Concerning the gap topology, scanning tunneling spectroscopy measurements point to a fully open gap, with some anisotropy on the Fermi surface.⁹ The indication of unconventional superconductivity might come from the distribution of values of the residual density of states (at zero energy) on different parts of the sample surface. This could be attributed to a pair-breaking effect of disorder. The same conclusion as regards the gap size was reached by μ SR measurements¹⁰ and NQR measurements,¹¹ although unconventional superconductivity is suggested in the latter case by the absence of a coherence peak below T_c in $1/T_1$.

This should be contrasted with recent penetration depth measurements, that would indicate point nodes of the gap,¹²

or the angular dependence of the thermal conductivity which suggests an anisotropic superconducting gap with a nodal structure.¹³ This latter measurement also suggests multiple phases in the temperature (T) - field (H) plane, which could be connected to the double transition observed in a zero field.¹⁴⁻¹⁶ Recent μ SR relaxation experiments¹⁷ detected a broadening of the internal field distribution below T_c , suggesting a multicomponent order parameter or a nonunitary odd parity state, with a finite magnetic moment.

In this context, our results bring new insight on the question of the parity of the order parameter, and draw a definite picture of the (H, T) low field phase diagram as deduced from specific heat measurements. With reference to the historical case of UPt₃, we emphasize that the present status of the sample quality may explain the discrepancies between the various measurements: definite claims on the nature of the superconducting state in PrOs₄Sb₁₂ are at the very best too early, the key point being the sample quality.

II. EXPERIMENTAL DETAILS

We present results on single crystals of PrOs₄Sb₁₂ grown by the Sb flux method.¹⁸⁻²⁰ These samples are aggregates of small single crystals with well developed cubic faces. They have a good RRR of about 40 (between room temperature and 2 K), a superconducting transition (onset of C_p or ρ) at 1.887 K and, they present a very sharp double superconducting transition in the specific heat.

Two different techniques have been used for the specific heat measurements. The first is a quasi-adiabatic method with a Au/Fe-Au thermocouple controlled by a superconducting quantum interference device (SQUID) in a ³He calorimeter. It is well suited to quantitative studies in the zero field (the addenda are precisely known), and was used on samples with a total mass of 8 mg. The second technique was ac calorimetry, used to follow the superconducting transitions under magnetic field in order to draw a complete phase diagram of the two superconducting transitions. This ac calorimetry uses a strain gauge heater (PtW alloy), a sensitive SiP thermometer (silicon doped with phosphorus close to the critical concentration of the metal-insulator transition),

and a long gold wire (25 μm diameter) as a heat leak. For the ac method, we choose a frequency of 0.04 Hz and a large integration time of 350 s. The SiP thermometer is measured with a four lead resistance bridge at 500 Hz, whose analog output is sent to the lock-in detection. The heating power was chosen so that the SiP temperature oscillations remain smaller than 6 mK in order to avoid broadening of the transitions. Thermometry under field was controlled by thermometers located in the (zero field) compensated region of the magnet.

III. SPECIFIC HEAT RESULTS

Figure 1 displays the specific heat $C_p(0,T)/T$ of 3 samples of the same batch measured together, of total mass 8 mg. The inset of Fig.1 is the ac specific heat $C_p(0,T)$ of one of these three samples (hereafter called sample No. 1). As it has been previously observed,¹ $\text{PrOs}_4\text{Sb}_{12}$ shows a Schottky anomaly with a maximum in C_p/T near $T=2.2$ K. Absolute values of C_p/T are the highest ever reported: at $T=1.7$ K, $C_p/T=3.65$ J/K² mol and at $T=2$ K, $C_p/T=2.9$ J/mol K². Sample No. 1 has a well defined double transition: to our knowledge, it is the sharpest ever reported in the literature, although we are aware of similar (yet unpublished) results by Aoki²¹ on samples grown in the same group. The width of the two transitions was estimated to be 16 mK and 58 mK, with, respectively, $T_{c2}=1.716$ K and $T_{c1}=1.887$ K (with the junction criterion).

Shown in Figs. 2 and 3 are the ac specific heat measurements $C_p(H,T)$ at, respectively, constant magnetic field ($T_{c1} \geq 1.16$ K) and constant temperature ($T_{c1} \leq 1.15$ K) of the same sample No. 1. The normal state specific heat, or an arbitrary line between the two transitions, has been subtracted for the temperature or field sweeps, respectively. Even under the field, the transitions remain very sharp, so that we were able to detect them down to 350 mK and to draw a precise phase diagram (Fig. 4). The width of the two

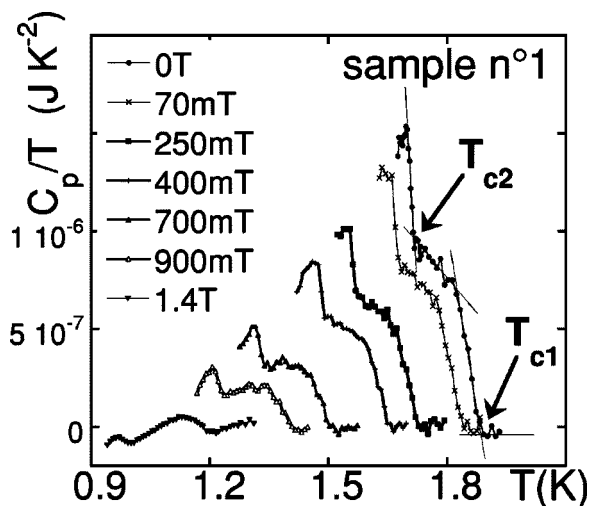


FIG. 2. Temperature sweeps of the ac specific heat of sample No. 1 at several fields below 1.4 T. The normal state was subtracted. The arrows indicate the double transition T_{c1} and T_{c2} .

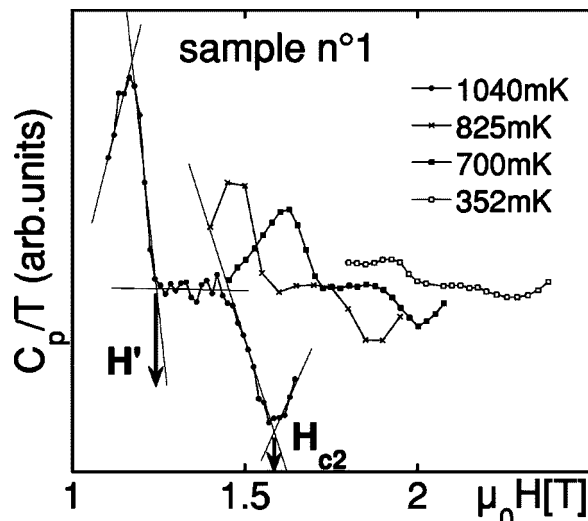


FIG. 3. Field sweeps of the ac specific heat of sample No. 1 at several temperatures. An arbitrary line between the two transitions was subtracted. We follow the two transitions (H_{c2} and H') down to 350 mK.

transitions does not exceed $\Delta H_{c2}=80$ mT and $\Delta H'=50$ mT at 500 mK, and $\Delta T_{c1}=35$ mK and $\Delta T_{c2}=70$ mK at 1.4 T.

The low field phase diagram has the same features as reported by Tayama *et al.*⁵ from magnetization measurements. The advantage of specific heat is to give an unambiguous signature of a bulk phase transition, that cannot be confused with other physical phenomena like a peak-effect. The two transition lines remain almost parallel and we will see that they can be deduced from each other simply by scaling T_c .

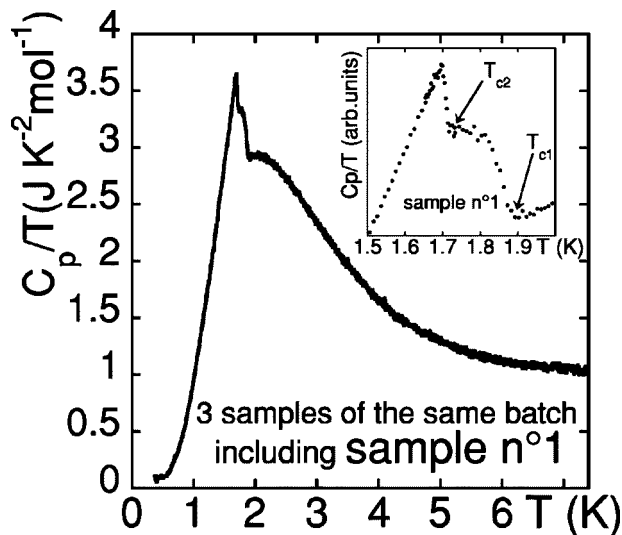


FIG. 1. Specific heat of samples of the same batch including sample $n^{\circ}1$ as C_p/T versus T at the zero field measured with a quasi-adiabatic method. The inset is a zoom on the double superconducting transition of sample No. 1 measured with an ac method: $T_{c1}=1.887$ K and $T_{c2}=1.716$ K.

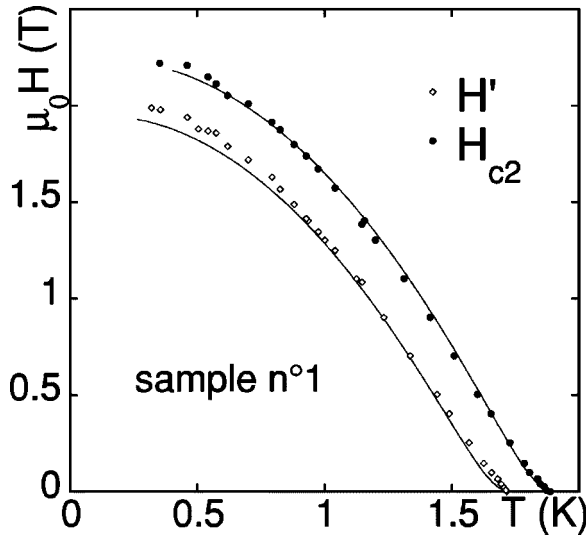


FIG. 4. H - T superconducting phase diagram of $\text{PrO}_4\text{Sb}_{12}$ determined by specific heat measurements on sample No. 1. The field dependence of T_{c1} and T_{c2} are completely similar. The lines are fits by a two-band model of the upper critical field (Sec.V B 2). Only T_c has been changed from H_{c2} to H' .

IV. SAMPLE CHARACTERIZATION

Three pieces of sample No. 1 have been used for further characterizations, called 1a, 1b and 1c. As well as the specific heat of sample No. 1a (2 mg), we have measured the resistivity of samples No. 1b (0.2 mg) and No. 1c, and the ac susceptibility and dc magnetization of samples No. 1a and No. 1b.

Concerning the specific heat, the high absolute value of C_p as well as the large height of the two superconducting jumps [$\Delta(C_p/T)=350$ mJ/mol. K^2 at T_{c1} and $\Delta(C_p/T)=300$ mJ/mol K^2 at T_{c2}] must be linked to the high quality of these samples (the absence of Sb-flux and/or good stoichiometry). Moreover, the heights of the two steps of sample No. 1a are quantitatively similar to those of the entire batch (7.5 mg) as Vollmer has already pointed out.¹⁴

Like in previous work,^{1,22} we have noticed that the resistivity at 300 K is very sample dependent (from 200 to 900 $\mu\Omega$ cm). On all samples, the value of ρ at 300 K seems to scale with the slope at high temperature ($T \geq 200$ K), i.e., the phononic part of the resistivity, as if the discrepancies were due to an error on the geometric factor. This error could be explained by the presence of microcracks in the samples. We have taken this problem into account by normalizing all data to the slope $d\rho/dT$ at high temperature ($T \geq 200$ K) of sample No. 1c, chosen arbitrarily. For samples No. 1b and No. 1c, respectively (Fig. 5), the RRR (ratio between 300 K and 2 K values) are 44 and 38, the onset T_c are 1.899 K and 1.893 K (matching the critical temperature obtained by specific heat), and the temperatures of vanishing resistance ($T_{R=0}$) are 1.815 K and 1.727 K. $T_{R=0}$ of sample No. 1c is equal to T_{c2} and this remains true under a magnetic field. So, in sample No. 1c, the resistive superconducting transition is not complete between T_{c1} and T_{c2} .

Figure 6 shows the superconducting transition for samples No. 1a and No. 1b by ac-susceptibility ($H_{ac}=0.287$ Oe), cor-

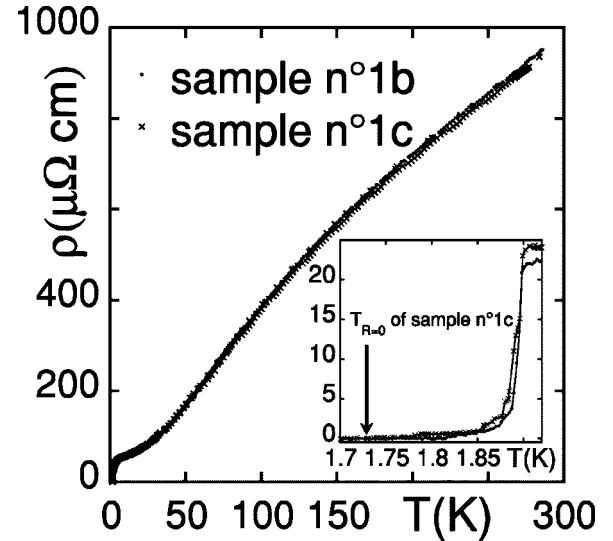


FIG. 5. Resistivity of samples No. 1b and No. 1c normalized to the slope at high temperature of sample No. 1c. The inset is a zoom on the superconducting transition. The resistivity of sample No. 1c is zero only at T_{c2} .

rected for the demagnetization field. The onset temperature is the same for the two samples (1.88 K). The transition is complete only at around 1.7 K and two transitions are visible. The field cooled dc magnetization of samples No. 1a and No. 1b ($H_{dc}=1$ Oe), shown in Fig. 7, gives a Meissner effect of, respectively, 44% and 55%, indicating (like specific heat) that the superconductivity is bulk. The two transitions are also visible.

V. DISCUSSION

A. Double superconducting transition

Let us first discuss the nature (intrinsic or not) of the double transition observed in our specific heat measure-

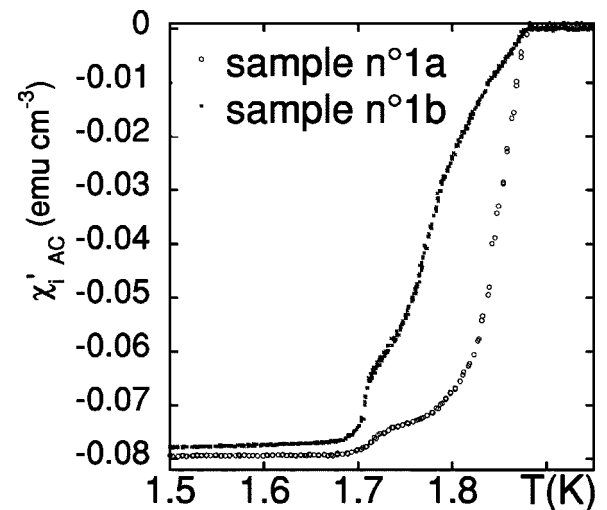


FIG. 6. The real part χ'_1 of the ac susceptibility of samples No. 1a and No. 1b measured with an ac magnetic field of 0.287 Oe at 2.11 Hz. Like in the results of resistivity measurement, the superconducting transition is not complete at T_{c1} and the two transitions are visible.

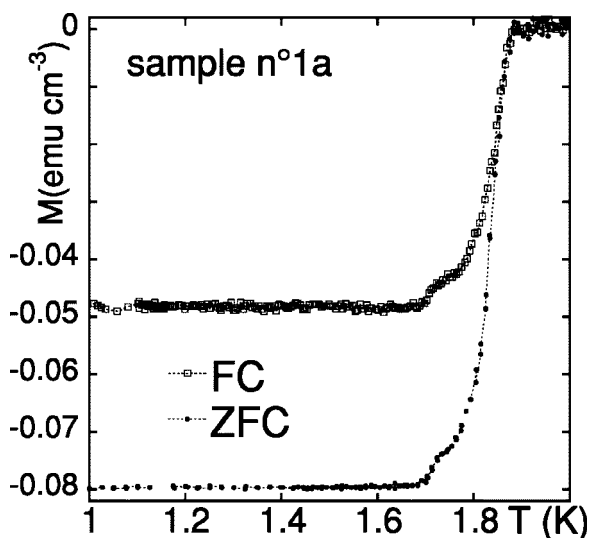


FIG. 7. dc magnetization of sample $n^\circ 1a$ at $H_{DC}=1$ Oe with zero field cooled (ZFC) and field cooled (FC) sweeps. The Meissner effect is 44% for this sample and 55% for sample No. 1b (not shown). The superconductivity is bulk.

ments. The remarkable fact, compared to previous reports,^{14,15} is the progress on the sharpness of both transitions. If for previous reports, a simple distribution of T_c due to a distribution of strain in the sample could have explained the transition width, it is not the case anymore for the sharp features observed on these new samples. Also the explanation recently proposed²³ that the lower transition at T_{c2} would be induced by Josephson coupling of one sheet of the Fermi surface to another with transition temperature T_{c1} is excluded, owing to the sharpness of both transitions and particularly of that at T_{c2} : see the broadening calculated by the authors²³ for the Josephson induced transition. Nevertheless, some of our results still cast serious doubts on the intrinsic nature of the double transition. Indeed, the susceptibility also shows a “double” transition, and resistivity becomes zero only at T_{c2} . If the first transition at T_{c1} was bulk-homogeneous, the resistivity should immediately sink to zero below T_{c1} , and the susceptibility (χ) should also show perfect diamagnetism far before T_{c2} : the sample diameter is at least 1000 times larger than the penetration depth (λ) so that the temperature dependence of λ cannot explain such a transition width of χ (contrary to the statements of Chia¹²). So both resistivity and susceptibility are indicative of remaining sample inhomogeneities.

Nevertheless, in our opinion, even the comparison of the various characterizations of the superconducting transition by resistivity, susceptibility and specific heat on the same sample does not allow for a definite conclusion.

Two historical cases are worth remembering. URu_2Si_2 showed a double transition in the specific heat in some samples, with inhomogeneous features detected in the susceptibility.²⁴ In that case, the authors of Ref. 24 could clearly show that it was not intrinsic (maybe arising from internal strain ?) because different macroscopic parts of the same sample showed one or the other transition. In $PrOs_4Sb_{12}$, the specific heat results are reproducible among

various samples of the same batch (see samples No. 1 and No. 1a of the present work), and such an easy test does not work.

The second case is of course UPt_3 : it is now well established that the two transitions observed in the zero field are intrinsic and correspond to order parameters of different symmetries. But the first results on samples that were not homogeneous enough showed exactly the same behavior as the present one in $PrOs_4Sb_{12}$: two features in the susceptibility and a very broad (covering both transitions) resistive transition.²⁵ It was not until the sample quality improved significantly that resistivity and susceptibility transitions matched the higher one.²⁶ The puzzling result for $PrOs_4Sb_{12}$, compared to UPt_3 , is that despite the sharpness of the specific heat transitions, resistivity and susceptibility reveal inhomogeneities, which means that this new compound probably has unusual metallurgical specificities.

Continuing the parallel with UPt_3 , basic measurements rapidly supported the intrinsic origin of the two transitions: they were probing the respective field and pressure dependence of both transitions. Indeed, a complete (H-T) phase diagram was rapidly drawn, showing that in UPt_3 ,²⁷ like in $U_{1-x}Th_xBe_{13}$,²⁸ the two transitions observed in the zero field eventually merged under a magnetic field, due to a substantial difference in dT_c/dH . It is even more true for the pressure dependence of $T_{c1,2}$, as the thermal dilation has jumps of opposite sign at the two transitions, indicating opposite variations of $T_{c1,2}$ under pressure (Ehrenfest relations).²⁹ So in this compound, the two transitions could be rapidly associated with a change of the symmetry of the order parameter indicating the unconventional nature of the superconducting state.

We are not so lucky in the case of $PrOs_4Sb_{12}$: indeed, the field dependence of T_{c2} seems completely similar to that of T_{c1} (Fig. 4), a claim that will be made quantitative below. It is the same situation as in URu_2Si_2 ,²⁴ and nothing in favor of an intrinsic nature of the double transition can be deduced from this phase diagram. Another phase diagram has already been established by transport measurements, with a line $H^*(T)$ separating regions of twofold and fourfold symmetry in the angular dependence of thermal conductivity under magnetic field.¹³ It may seem likely^{13,30} that this line would merge with the double transition in the zero field. From the line $H'(T)$ drawn from our specific heat measurements [$T_{c2}(H)$, Fig. 4], we can conclude that this is not the case: $H'(T)$ does not match the line $H^*(T)$ drawn in Ref. 13, unless there is an unlikely strong sample dependence of these lines.

A comparison of the pressure dependence of T_{c1} and T_{c2} seems more promising: contrary to case of UPt_3 ,²⁹ the jump of the thermal expansion at the two superconducting temperatures does not change sign,¹⁶ but from the relative magnitude of these jumps and our specific heat peaks, we get a value $dT_{c1}/dp \approx -0.2$ K/GPa, and twice as much for dT_{c2}/dp . This supports a different origin for both transitions. The weak point is that the thermal expansion measurements were done on two samples mounted on top of each other, which were early samples with rather broad specific heat transitions. Thus, the question of the intrinsic nature of the double superconducting transition remains open.

B. Upper critical field

Another quantity which has not been thoroughly discussed is the upper critical field $H_{c2}(T)$. In heavy fermion superconductors, $H_{c2}(T)$ has always proved to be an interesting quantity, mainly due to the large mass enhancement of the quasiparticles. Indeed, the usual orbital limitation is very high in these systems, due to the low Fermi velocity, so that the authors of Ref. 1 could, from their $H_{c2}(T)$ data, confirm the implication of heavy quasiparticles in the Cooper pairs (revealed also by the specific heat jump at T_c). They also gave an estimate of the heaviest mass: $\approx 50 m_0$, where m_0 is the free electron mass.

But, as the orbital limitation is very high, $H_{c2}(T)$ is also controlled by the paramagnetic effect. A quantitative fit of $H_{c2}(T)$ easily gives the amount of both limitations, except that on this system, $H_{c2}(T)$ has an extra feature: a small initial positive curvature close to T_c . This feature has been systematically found, whatever the samples and the techniques used to determine $H_{c2}(T)$ (ρ , χ and C_p).^{1,13,14,22} Our data, obtained by ρ on sample No. 1c and C_p on sample No. 1, matches all other published results. So we can now consider this curvature of $H_{c2}(T)$ as intrinsic, and not due to some artifact of transport measurements, or coming from inhomogeneity in the sample. Such an intrinsic positive curvature also appears in MgB_2 ³¹ or in borocarbides like $\text{YNi}_2\text{B}_2\text{C}$ and LuNi_2B_2 .³²

1. Physical inputs

We propose an explanation based on different gap amplitudes for the different sheets of the Fermi surface of $\text{PrOs}_4\text{Sb}_{12}$, which is made quantitative through a “two-band” model.³³ Microscopically, STM spectroscopy also reveals an anisotropic gap, with zero density of states at low energy (fully open gap) but a large smearing of the spectra.⁹ Recent microwave spectroscopy measurements also discuss a two band model,²³ but in order to explain the double transition. We insist that our model has nothing to do with the double transition, which clearly involves heavy quasiparticles both at T_{c1} and at T_{c2} (see the size of the two specific heat jumps): our aim is a quantitative understanding of $H_{c2}(T)$, based on the normal state properties of $\text{PrOs}_4\text{Sb}_{12}$, as in MgB_2 or borocarbides where no double transition has ever been observed. The physical input of a multi-band model for $H_{c2}(T)$ is to introduce different Fermi velocities and different inter and intra band couplings. As a result, T_c is always larger than for any of the individual bands.³⁴ The slope of H_{c2} at T_c is larger for slower Fermi velocity (heavier) bands. Positive curvature of $H_{c2}(T)$ is easily obtained if the strongest coupling is in the heaviest bands (large H_{c2}), with a slight T_c increase due to the inter band coupling to the lightest bands (small initial slope).³²

2. The two-band model

There are at least three sheets for the Fermi surface of $\text{PrOs}_4\text{Sb}_{12}$, but in the absence of a precise knowledge of the pairing interaction, a full model would be unrealistic, having an irrelevant number of free parameters. A two-band model

is enough to capture the physics of anisotropic pairing, although only the correspondence with band calculations becomes looser. In our model, band 2 would correspond to the lightest (β) band detected by de-Haas van Alphen measurements, and band 1 would be a heavy band having most of the density of states. Indeed, the de Haas-van Alphen experiments on $\text{PrOs}_4\text{Sb}_{12}$ ^{18,35} reveal the presence of light quasiparticles (band β) and heavier particles (band γ). The heaviest quasiparticles are at present only seen by thermodynamic measurements (C_p or H_{c2}). Anisotropic coupling between the quasiparticles is considered in the framework of an Eliashberg strong coupling two-band model³³ in the clean limit, with an Einstein phonon spectrum (characteristic “Debye” frequency Ω). Let us point out that the results do not depend on (and *a fortiori* do not probe) the pairing mechanism, which is likely to be much more exotic than the usual electron-phonon mechanism. Compared to a single band calculation, there is now a matrix of strong coupling parameters λ_{ij} describing the diffusion of electrons of band i to band j by the excitations responsible for the pairing (see the Appendix for detailed equations).

What matters for $H_{c2}(T)$ is the relative weight of the λ_{ij} , not their absolute value: we consider T_c or the renormalized Fermi velocities as experimental inputs. λ_{ij} depends both on the interaction matrix elements between bands i and j , and on the final density of states of band j .³⁴ In MgB_2 , it is claimed that electron-phonon coupling is largest within the σ bands. Here, knowing nothing about the pairing mechanism, we assume constant inter and intra band coupling, so that the relative weight of the λ_{ij} is only governed by the density of states of band j . This density of states is itself proportional to the contribution of that band to the specific heat Sommerfeld coefficient: 500 mJ/K² mol¹ for band 1, 20 mJ/K² mol for band 2.^{18,35} The Fermi velocity of band 1 (not observed by de Haas-van Alphen measurements) is the main adjustable parameter of the fit: we find $v_{F1}=0.0153 \times 10^6$ m.s⁻¹, in agreement with Ref. 1 where the Fermi velocity has been inferred from the slope of $H_{c2}(T)$ at T_c ignoring the initial positive curvature. All other coefficients are either arbitrary ($\lambda_{1,1}=1$) (in agreement with the strong coupling superconductivity concluded in Ref. 11), conventional values (gyromagnetic ratio for the paramagnetic limitation $g=2$, Coulomb repulsion parameter $\mu_{i,j}^*=0.1 \delta_{i,j}$), or fixed by experimental data ($T_c=1.887$ K $\Rightarrow \Omega=21.7$ K, $v_{F2}=0.116 \times 10^6$ m.s⁻¹ from the de Haas-van Alphen data on the β band). The model fits well the experimental data (cf. Fig. 4), including the small positive curvature. Before discussing the interpretation of the fit as regards the values of the parameters and the parity of the superconducting order parameter, let us note that we can fit the $H'(T)$ line (Fig. 4) with the same parameters as for H_{c2} except Ω , adjusted to give $T_c=1.716$ K. There is a good agreement with all data except at very low temperature or near T_c where the curvature is reduced compared to $H_{c2}(T)$. However, these deviations are weak, and this is why we claim that $H'(T)$ has the same behavior as $H_{c2}(T)$, which does not help to identify the second transition with a symmetry change of the superconducting order parameter.

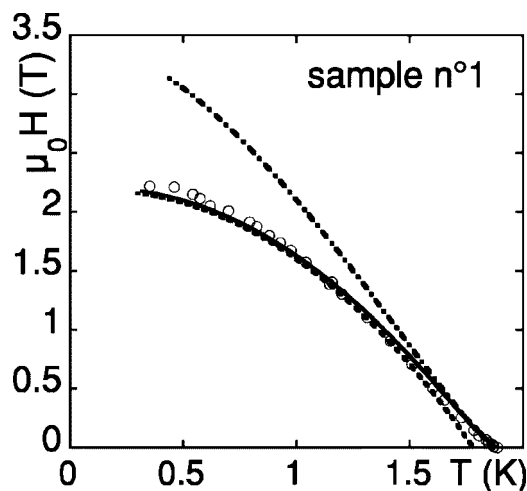


FIG. 8. Open circles show the data of $H_{c2}(T)$ by specific heat measurement on $\text{PrOs}_4\text{Sb}_{12}$ (sample No. 1). The lines show fits with a two-band model (solid line), with a single band model (dashed line), without the paramagnetic limit ($g=0$) (dotted line). It shows that the increase of T_c due to the coupling with light qp band is rapidly suppressed in weak magnetic fields. H_{c2} is also clearly Pauli limited, supporting a singlet superconducting state. The parameters for the solid line fit are $g=2$, $\mu_{ij}^*=0.1\delta_{ij}$, $v_{F1}=0.0153 \times 10^6 \text{ m}\cdot\text{s}^{-1}$ (heavy band), $v_{F2}=0.116 \times 10^6 \text{ m}\cdot\text{s}^{-1}$ (lightest band, from de Haas-van Alphen oscillations) [Ref. 18], $T_c=1.887 \text{ K} \Rightarrow \Omega=21.7 \text{ K}$.

3. Interpretation

Shown also in Fig. 8 are the calculations of $H_{c2}(T)$ for a single band model: v_{F1} , the characteristic frequency Ω and $\lambda_{1,1}$ have the same values as before, but all other λ_{ij} coefficients have been turned down to zero, eliminating the effects of the light electron band. T_c is then reduced (down to 1.78 K) and the positive curvature disappears. We also observe that the fit of H_{c2} is basically unchanged above 1 T, meaning that low fields suppress the superconductivity due to the light electron band restoring a “single band” superconducting state. This is the same effect observed more directly in MgB_2 with specific heat measurements under magnetic field: the smaller gap rapidly vanishes, leading to a finite density of states at the Fermi level under magnetic fields due to the π band.³⁶ This suppression of the light quasiparticle superconductivity would have here an effect on specific heat too small to be observed (contribution of the light quasiparticles to the specific heat of order 4% of the Sommerfeld coefficient, itself buried in the large Schottky anomaly). But it may have much larger effects on transport. Let us note that the clean limit is *a posteriori* justified: from v_{F1} , we find a coherence length $\xi_0 \sim 110 \text{ \AA}$, whereas from a residual resistivity ρ_0 and specific heat coefficient $\gamma \sim 0.5 \text{ J/K}^2 \text{ mol} \sim 2 \times 10^3 \text{ J/K}^2 \text{ m}^3$, we get $v_{F1}l \sim 3L_0/\rho\gamma \sim 2 \times 10^{-3} \text{ m}^2/\text{s}$ yielding a mean free path $l \sim 1300 \text{ \AA} > 10 \xi_0$.

More interestingly, the quantitative fit of H_{c2} also allows a discussion of the parity of the order parameter in $\text{PrOs}_4\text{Sb}_{12}$. Indeed, like other heavy fermion superconductors, despite the low- T_c value, H_{c2} can be sensitive to the Pauli limit in case of singlet pairing. The fit in Fig. 8 includes this para-

magnetic limitation, with the conventional free electron value for g ($g=2$). Also shown in Fig. 8 is the calculation of $H_{c2}(T)$ with the same parameters but for $g=0$, i.e., without any paramagnetic limit. The strong deviations observed demonstrate that the paramagnetic effect controls H_{c2} at low temperature in $\text{PrOs}_4\text{Sb}_{12}$. Quantitatively, the paramagnetic effect depends on the coupling strength. Yet, we choose arbitrarily $\lambda=1$. A rather strong coupling regime is supported by *NQR* experiments.¹¹ Even for a weak coupling picture ($\lambda=0.6$), the fit yields $g=1.55$. In both cases, the paramagnetic limit remains important, supporting a singlet nature of the superconductivity, contrary to what had been suggested in Ref. 37–39 and in agreement with the supposition in Ref. 7 and 30. This result should be quite robust, independent of the two-band model. It could be invalidated if the mass renormalization mechanism was field dependent, which could be an explanation for the difference in the large specific heat Sommerfeld coefficient obtained in the low field, and the de Haas-van Alphen measurements performed at a high field.⁸ In such a case, the “saturation” of $H_{c2}(T)$ at low temperature could arise from a reinforcement of the orbital limitation alone.

VI. CONCLUSION

To conclude, we have drawn a very precise superconducting phase diagram of $\text{PrO}_4\text{Sb}_{12}$ down to 350 mK, by a specific heat measurement. We have yet no clear evidence of the unconventional nature of the superconducting order parameter from this phase diagram. The superconducting phase diagram with the symmetry change of the order parameter drawn by Izawa *et al.*¹³ from transport measurements does not seem related to the double transition observed with specific heat measurements. Despite the high quality of the sample, we cannot completely exclude that there are still two parts with different T_c in our sample, as $H'(T)$ is just scaled from H_{c2} with respect to T_c . The puzzling result is that despite sharp specific heat transitions, inhomogeneities are still present in the samples. This calls for caution in the claim of various types of nodes of the gap by different sophisticated techniques: the most urgent task is to understand the problem of sample quality. In contrast the upper critical field is very reproducible, independent of samples and types of measurements. It has been analyzed with a strong coupling two-band model taking into account the spread in the effective masses of the quasi-particles and of the pairing strength as suggested also by STM spectroscopy measurements.⁹ The strong influence of the paramagnetic limit on H_{c2} is the first experimental argument for a singlet superconducting order parameter.

ACKNOWLEDGMENTS

We acknowledge many fruitful discussions with K. Izawa, H. Harima, V. Mineev, H. Suderow, J-L. Tholence, P.C. Canfield, and G. Lapertot. This research was supported by the Grant-in Aid for Scientific Research on the Priority Area “Skutterudites” from MEXT in Japan.

APPENDIX: THE TWO-BAND MODEL

Equations for two band superconductors have been given by numerous authors.³²⁻³⁴ For the sake of completeness, here we give the linearized gap equations under a magnetic field, for a superconductor in the clean limit (negligible impurity scattering), as can be found in Ref. 32 [with corrections of typewriting mistakes of factor 2 in the Matsubara frequency and definition of $\lambda_{i,j}(n)$]. In the following, i and j are the band index, $\alpha_{i,j}F(\omega)$ is the density of interactions from band i to j (involving diffusion from band i to j), v_{Fi} is the Fermi velocity of band i and H_{c2} is the upper critical field:

$$\begin{aligned} \tilde{\Delta}_i(n) &= \pi T \sum_{j,m} [\lambda_{i,j}(m-n) - \mu^* \delta_{i,j} \theta(\omega_c - |\omega_m|)] \\ &\quad \times \chi_j(m) \tilde{\Delta}_j(m)(\omega_m), \\ \tilde{\omega}_i(n) &= \omega_n + \pi T \sum_{j,m} [\lambda_{i,j}(m-n)] \text{sgn}(\omega_m), \\ \chi_i(n) &= (2/\sqrt{\beta_i}) \int_0^\infty dq \exp(-q^2) \\ &\quad \times \tan^{-1} \left\{ \frac{q\sqrt{\beta_i}}{[|\tilde{\omega}_i(n)| + i\mu_B H_{c2} \text{sgn}(\omega_n)]} \right\}, \quad (\text{A1}) \end{aligned}$$

with

$$\beta_i = \pi H_{c2} v_{Fi}^2 / (2\phi_0), \quad \omega_n = \pi T(2n+1),$$

$$\lambda_{i,j}(n-m) = 2 \int_0^\infty d\omega \alpha_{i,j}^2 \omega \frac{F(\omega)}{\omega^2 + (\omega_n - \omega_m)^2}.$$

The value of H_{c2} is given by the largest set of values of β_i yielding a nontrivial solution of Eq. (A1).

We have used in addition an Einstein spectrum for the density of interactions:

$$\alpha_{i,j}(\omega)F(\omega) = \frac{\lambda_{i,j}\Omega}{2} \delta(\omega - \Omega),$$

introducing a characteristic energy scale Ω . In the calculations, we find $\Omega \approx 21$ K: let us note that in reality, this value of Ω remains undetermined, as it depends directly of the absolute value of the $\lambda_{i,j}$ whereas the shape of H_{c2} is controlled only by the relative size of the $\lambda_{i,j}$ (as long as they are not too large). Nevertheless, a rather small value of ω is indeed possible in heavy-fermion systems, because the heavy fermion state is precisely occurring due to the presence of small energy scales. The cut-off parameter ω_c in Eq. (A1) is taken to 10Ω , and the infinite system of Eq. (A1) has been truncated at each temperature when $|\omega_n|$ reaches ω_c .

Eventually, let us note that bare Fermi velocities enter the above equations, and that renormalized Fermi velocities: $v_{Fi}^* = v_{Fi} / (1 + \sum_j \lambda_{i,j})$ should be used for comparison to specific heat or de Haas-van Alphen measurements.³⁴

-
- ¹E. D. Bauer, N. A. Frederick, P.-C. Ho, V. S. Zapf, and M. B. Maple, Phys. Rev. B **65**, 100506(R) (2002).
²K. Takegahara, H. Harima, and A. Yanase, J. Phys. Soc. Jpn. **70**, 1190 (2001).
³M. Kohgi, K. Iwasa, M. Nakajima, N. Metoki, S. Araki, N. Bernhoeft, J.-M. Mignot, A. Gukasov, H. Sato, Y. Aoki, and H. Sugawara, J. Phys. Soc. Jpn. **72**, 1002 (2003).
⁴Y. Aoki, T. Namiki, S. Ohsaki, S. R. Saha, H. Sugawara, and H. Sato, J. Phys. Soc. Jpn. **71**, 2098 (2002).
⁵T. Tayama, T. Sakakibara, H. Sugawara, Y. Aoki, and H. Sato, J. Phys. Soc. Jpn. **72**, 1516 (2003).
⁶C. R. Rotundu, H. Tsujii, Y. Takano, B. Andraka, H. Sugawara, Y. Aoki, and H. Sato, Phys. Rev. Lett. **92**, 037203 (2004).
⁷K. Maki, H. Won, P. Thalmeier, Q. Yuan, K. Izawa, and Y. Matsuda, Europhys. Lett. **64**, 496 (2003).
⁸H. Harima (private communication).
⁹H. Suderow, S. Vieira, J. D. Strand, S. Bud'ko, and P. C. Canfield, Phys. Rev. B **69**, 060504 (2004).
¹⁰D. E. MacLaughlin, J. E. Sonier, R. H. Heffner, O. O. Bernal, B. L. Young, M. S. Rose, G. D. Morris, E. D. Bauer, T. D. Do, and M. B. Maple, Phys. Rev. Lett. **89**, 157001 (2002).
¹¹H. Kotegawa, M. Yogi, Y. Imamura, Y. Kawasaki, G.-q. Zheng, Y. Kitaoka, S. Ohsaki, H. Sugawara, Y. Aoki, and H. Sato, Phys. Rev. Lett. **90**, 027001 (2003).
¹²E. E. M. Chia, M. B. Salamon, H. Sugawara, and H. Sato, Phys. Rev. Lett. **91**, 247003 (2003).
¹³K. Izawa, Y. Nakajima, J. Goryo, Y. Matsuda, S. Osaki, H. Sugawara, H. Sato, P. Thalmeier, and K. Maki, Phys. Rev. Lett. **90**, 117001 (2003).
¹⁴R. Vollmer, A. Faißt, C. Pfeleiderer, H. v. Löhneysen, E. D. Bauer, P.-C. Ho, V. Zapf, and M. B. Maple, Phys. Rev. Lett. **90**, 057001 (2003).
¹⁵M. B. Maple, P.-C. Ho, V. S. Zapf, N. A. Frederick, E. D. Bauer, W. M. Yuhasz, F. M. Woodward, and J. W. Lynn, J. Phys. Soc. Jpn. **71** Suppl., 23 (2002).
¹⁶N. Oeschler, P. Gegenwart, F. Steglich, N. A. Frederick, E. D. Bauer, and M. B. Maple, Acta Phys. Pol. B **34**, 959 (2003).
¹⁷Y. Aoki, A. Tsuchiya, T. Kanayama, S. R. Saha, H. Sugawara, H. Sato, W. Higemoto, A. Koda, K. Ohishi, K. Nishiyama, and R. Kadono, Phys. Rev. Lett. **91**, 067003 (2003).
¹⁸H. Sugawara, S. Osaki, S. R. Saha, Y. Aoki, H. Sato, Y. Inada, H. Shishido, R. Settai, Y. Onuki, H. Harima, and K. Oikawa, Phys. Rev. B **66**, 220504(R) (2002).
¹⁹N. Takeda and M. Ishikawa, Physica B **259-261**, 92 (1999).
²⁰E. D. Bauer, A. Ślebarski, E. J. Freeman, C. Sirvent, and M. B. Maple, J. Phys.: Condens. Matter **13**, 4495 (2001).
²¹Y. Aoki (private communication).
²²P.-C. Ho, N. A. Frederick, V. S. Zapf, E. D. Bauer, T. D. Do, M. B. Maple, A. D. Christianson, and A. H. Lacerda, Phys. Rev. B **67**, 180508 (2003).
²³D. M. Broun, P. J. Turner, G. K. Mullins, D. E. Sheehy, X. G. Zheng, S. K. Kim, N. A. Frederick, M. B. Maple, W. N. Hardy, and D. A. Bonn, cond-mat/0310613 (unpublished).
²⁴A. P. Ramirez, T. Siegrist, T. T. M. Palstra, J. D. Garrett, E.

- Bruck, A. A. Menovsky, and J. A. Mydosh, *Phys. Rev. B* **44**, 5392 (1991).
- ²⁵A. Sulpice, P. Gandit, J. Chaussy, J. Flouquet, D. Jaccard, P. Lejay and J. L. Tholence, *J. Low Temp. Phys.* **62**, 39 (1986).
- ²⁶K. Hasselbach, L. Taillefer, and J. Flouquet, *Phys. Rev. Lett.* **63**, 93 (1989).
- ²⁷G. Bruls, D. Weber, B. Wolf, P. Thalmeier, B. Lüthi, A. de Visser, and A. Menovsky, *Phys. Rev. Lett.* **65**, 2294 (1990); S. Adenwalla, S. W. Lin, Q. Z. Ran, Z. Zhao, J. B. Ketterson, J. A. Sauls, L. Taillefer, D. G. Hinks, M. Levy, and B. K. Sarma, *ibid.* **65**, 2298 (1990).
- ²⁸D. S. Jin, S. A. Carter, T. F. Rosenbaum, J. S. Kim, and G. R. Stewart, *Phys. Rev. B* **53**, 8549 (1996).
- ²⁹K. Hasselbach, A. Lacerda, K. Behnia, L. Taillefer, and J. Flouquet, *J. Low Temp. Phys.* **81**, 299 (1990).
- ³⁰J. Goryo, *Phys. Rev. B* **67**, 184511 (2003).
- ³¹S. L. Budko and P. C. Canfield, *Phys. Rev. B* **65**, 212501 (2002).
- ³²S. V. Shulga, S.-L. Drechsler, G. Fuchs, K.-H. Müller, K. Winzer, M. Heinecke, and K. Krug, *Phys. Rev. Lett.* **80**, 1730 (1998).
- ³³M. Prohammer and E. Schachinger, *Phys. Rev. B* **36**, 8353 (1987).
- ³⁴I. I. Mazin and V. P. Antropov, *Physica C* **385**, 49 (2003).
- ³⁵H. Sugawara, S. Osaki, S. R. Saha, Y. Aoki, and H. Sato, *Acta Phys. Pol. B* **34**, 1125 (2003).
- ³⁶F. Bouquet, Y. Wang, I. Sheikin, T. Plackowski, A. Junod, S. Lee, and S. Tajima, *Phys. Rev. Lett.* **89**, 257001 (2002).
- ³⁷F. B. Anders, *Eur. Phys. J. B* **28**, 9 (2002).
- ³⁸K. Miyake, H. Kohno, and H. Harima, *J. Phys.: Condens. Matter* **15**, L275-84 (2003).
- ³⁹M. Ichioka, N. Nakai, and K. Machida, *J. Phys. Soc. Jpn.* **72**, 1322 (2003).